Inhaled Crocidolite Mutagenicity in Lung DNA

Bertrand Rihn,[1] Catherine Coulais,[1] Edmond Kauffer,[1] Marie-Claire Bottin,[1] Patrick Martin,[1] Francois Yvon,[1] Jean Claude Vigneron,[1] Stéphane Binet,[1] Nathalie Monhoven,[2] Guy Steiblen,[3] and Gérard Keith[3]

[1]Institut National de Recherche et de Sécurité, Vandoeuvre, France; [2]Laboratoire de Biologie Moléculaire de l'Hôpital Central de Nancy, Nancy, France; [3]Unité Propre de Recherche 9002 du CNRS, Strasbourg, France

We used transgenic mice carrying the *lacI* reporter gene to study the mutagenesis potential of asbestos crocidolite. The animals were exposed by nose-only inhalation to an aerosol containing 5.75 mg/m^3 crocidolite dust for 6 hr/day and 5 consecutive days. After 1, 4, and 12 weeks, we examined four end points: the cytology of bronchoalveolar lavage, the lung load of crocidolite, the hydrophobic DNA adducts, and the mutations in the *lacI* reporter gene. Twelve weeks after exposure, nearly 10% of the inhaled fibers remained in the lung (227 ± 103 ng/mg lung). There was evidence of a typical inflammatory response consisting of multinucleate macrophages at weeks 4 and 12, whereas immediately after the exposure, we observed numerous polymorphonuclear neutrophils. The mutant frequency significatively increased during the fourth week after the exposure: 13.5×10^{-5} in the exposed group versus 6.9×10^{-5} in the control group. The induction factor, defined by the ratio of checked mutants of exposed mice to checked mutants of control mice, was 1.96. The mutation spectrum of control lung DNA and exposed lung DNA was similar, suggesting the possible involvement of a DNA repair decrease in crocidolite-treated animals. We used the ^{32}P-postlabeling method and did not detect any increase of either 5 mC or bulky adduct in treated mice. This is the first study that demonstrates asbestos mutagenicity *in vivo* after a nose-only inhalation. *Key words*: adduct, asbestos, crocidolite, lung DNA, *lacI* gene, macrophage, mutation, transgenic. *Environ Health Perspect* 108:341–346 (2000). [Online 23 February 2000]
http://ehpnet1.niehs.nih.gov/docs/2000/108p341-346rihn/abstract.html

Although the use of asbestos fibers has been banned in most industrialized countries, they are still a major environmental, occupational, and personal health concern. Asbestos fibers are considered tumorigenic and mutagenic for humans according to the U.S. Registry of Toxic Effects of Chemical Substances (*1*).

Physical dimension, biopersistence, surface reactivity, and fiber overload are all involved in the pathogenesis of asbestosis, bronchogenic carcinoma, and mesothelioma [reviewed by Kane (*2*)]. At the molecular level, oxidative stress and cytokine release by alveolar macrophages (AMs) and neutrophils are invoked in the pathogenesis of these illnesses (*2*).

Asbestos is thought to be a complete carcinogen (*3*), which means that it has the capability to initiate and promote tumors. Because asbestos fibers are not directly electrophilic, it has been proposed that asbestos is not a mutagenic compound per se (*4*). In fact, past *in vitro* studies have shown no mutagenic or weak mutagenic activity of asbestos samples [reviewed by Jaurand (*5*)]. Using the *Salmonella typhimurium* TA 102 oxidative stress sensitive strain, Faux et al. (*6*) showed mutagenicity induced by crocidolite, but not by chrysotile (chrysotile is the most-used asbestos worldwide). However, the mammalian cell paradigm found mutagenicity for both crocidolite and chrysotile at the S_1 locus (*7*) and for 50 µg/mL chrysotile at the *HLA-A* locus. Nevertheless, no mutagenicity was manifested at the *HPRT* locus (*7–9*) with crocidolite fibers. Furthermore, crocidolite induced a loss of heterozygosity *in vitro* at the *HLA-A* locus (*10*), as did chrysotile in Big Blue transgenic Rat 2λ cells (Stratagene, La Jolla, CA) at the λ locus (*11*).

Although many experiments have been performed *in vitro* to demonstrate the mutagenicity of asbestos (clastogenic effects and mitotic abnormalities), there is a lack of *in vivo* studies to assert this important property. Thus we investigated more extensively the *in vivo* mutagenesis potential, if any, of asbestos fibers. To our knowledge, no mutagenesis studies have been conducted on whole animals. We used a transgenic mouse system carrying the *lacI* reporter gene and investigated the effect of crocidolite fibers in a short-term assay. The animals were exposed by nose-only inhalation for 5 days, then four end points were analyzed: the inflammatory response of the lung, the lung burden of fibers, the DNA adduct formation, and the mutation rate as well as the position and the nature of the mutation on the *lacI* reporter gene induced by crocidolite fibers.

Materials and Methods

Mice. We obtained transgenic male *LacI* mice C57/Bl6 (lambda *LIZ*, BigBlue) from Stratagene. The mice were randomized and numbered by tattoo. The animals were housed in polycarbonate cages (1/cage) covered with spun-bonded polyester cage filters. The room temperature was 21 ± 1°C, and the pressure was 5 mm H_2O above the atmospheric pressure. The humidity ranged from 40 to 60% and a fluorescent light was on for 12 hr/day. The animals were fed with pellet food and water *ad libitum*. Two-month-old animals were exposed to the crocidolite aerosol; control animals were housed in nose-only exposure tubes without crocidolite during the experiment (6 hr/day for 5 days). We terminated the experiment 1, 4, or 12 weeks after the beginning of the exposure, depending on the animal group.

Exposure techniques. The crocidolite sample used in this study came from a batch (gift of R.E.G. Rendall, National Center for Occupational Health, Johannesburg, South Africa) that replaced the original Union Internationale Contre le Cancer (Geneva, Switzerland) sample when it ran out. The fiber size distribution of the gift batch is extensively described in a previous study (*12*). The elementary analysis of this crocidolite sample was checked by emission spectroscopy (ICAP 61E; Thermo Jarrell Ash, Franklin, MA). The result of the analysis, expressed as the mean of three determinations, in percent, was Mg, 1.49; Si, 22.8; Fe, 30.0; Mn, 0.097; Al, 0.05; Cr, < 0.002; and Ni, 0.017.

The fiber aerosol generator was previously described by Rihn et al. (*12*). In brief, the fibers were packed into a cylinder and pushed with a Teflon-coated piston on a steel brush. Clean air was provided by a six-bar compressor that delivered a 100-L/min air stream by an inverted cyclone device. The tangential position of the air inlet pipe gave the air flow a helicoidal movement from the top to the bottom of the cell to ensure the aerosol homogeneity. The aerosol concentrations were monitored online by photometry.

We used the chamber as previously described by Rihn et al. (*12*). Briefly, the

Address correspondence to B. Rihn, Institut National de Recherche et de Sécurité, Avenue de Bourgogne, BP 27 54501 Vandoeuvre Cédex, France. Telephone: 33 383 502 062. Fax: 33 383 508 711. E-mail: rihn@inrs.fr

We thank C. Marty, L. Delsaut, M. Villa, and C. Dubon for excellent technical assistance and C. Saliou for critical reading.

This study was partially supported by a grant (SE000482) of the Fondation pour la Recherche Médicale.

Received 27 July 1999; accepted 9 November 1999.

control process included measurements of the air flow, the depression, the temperature, and the humidity. We transferred all output signals to a computer, which processed sensor information, calculated regulation loops, and dispatched analogical tensions to the regulation valves. A second computer was connected to the first and was used to monitor the inhalation chamber conditions (air flow and relative humidity), the aerosol concentration, and the adjustments of the aerosol generator parameters. The temperature of the atmosphere was maintained between 20 and 22°C, the humidity between 40 and 60%, and the air volume exchange (100 L) was 60 times/hr. To avoid contamination of ambient air by inhalation of chamber pollutants, pressures inside the inhalation chamber and the glove box surrounding the chamber were maintained below the room pressure at 5 and 2.5 mm H_2O, respectively.

Animals were housed in transparent restraining tubes inserted in the inhalation chamber, a stainless concentric cylinder with a 48-tube capacity. The mice were continuously exposed nose only to the crocidolite aerosol (subjects) or to the ambient air (control mice). Small holes in each of the restraining tubes prevented hyperthermal effects. This flow-past design allowed each animal to breathe fresh crocidolite aerosol of well regulated particle concentration and size at all times; reinhalation of exhaled test atmosphere was minimized. The fraction of exhaled air in the chamber was < 1/1,000 on the basis of regular mouse breathing (25 mL/min/mouse) (*13*).

Atmosphere control. We determined the concentration of airborne dust by sampling on GF/C filters (Whatman International Ltd., Maidstone, UK) for 5–6 hr at a flow rate of 2 L/min. The sampling head was an open-faced Millipore cassette (Millipore, Bedford, MA). The weight of the filters before and after sampling was corrected according to the weight variations of three unexposed filters.

To determine the fiber number, we chose a short sampling period (5–10 sec) to avoid fiber amounts that were too high fiber and to avoid filter overload. We used 0.8-µm mixed ester cellulose membranes to sample the fibers, which were counted by phase-contrast microscopy (*12*). We assessed the fiber size distribution of either the aerosol or the bulk crocidolite sample by transmission electron microscopy (100CX; JEOL Ltd., Tokyo, Japan). For this measurement, the fibers were deposited on a Nucleopore (Millipore) filter covered with a thin layer of carbon.

To check the absence of contaminating metals produced by the generator, we also sampled dust on Whatman QM-A filters and analyzed by emission spectroscopy (ICAP 61E; Thermo Jarrell Ash, Franklin, MA).

Cytologic, histologic, and ultrastructural examinations. At the end of each time-point, we measured bronchoalveolar liquids by washing the lung 2 times with 500 µL phosphate buffered saline solution (pH 7.4). We determined the cell number after Trypan Blue (0.04% w/v) staining, and the nucleated cells were recorded in triplicate using a Thoma-Weiss counting cell (PolyLabs, Strasbourg, France). In addition, a portion of the bronchoalveolar liquid (100 µL) was spun for 5 min at 29*g* (Cytospin 2; Shandon, Pittsburgh, PA). The May Grünwald Giemsa staining was then performed and AMs, polymorphonucleated cells (PMC), and the lymphocytes (L) were counted. Our results are the mean of three independent measures.

For histologic observations, we fixed lung specimens from control and treated animals in Bouin's solution or in 4% (v/v) aqueous formalin solution, then embedded in paraffin, sectioned, stained with hematoxylin/eosin, and evaluated by adapting the Wagner scale as described previously (*12*) with an Ortoplan microscope (Leitz, Wetzlar, Germany).

To evaluate the fiber burden in the lungs, we cleaned the frozen left lobe of four control and four treated animals in acetone to remove the fat, dried them to constant weight, and reduced them to ashes in a low-temperature oven (150°C) for 2 hr. The ashes were gently homogenized in ultrapure water by handshaking, then filtered over a carbon-covered Nucleopore membrane (25 mm diameter, 0.4 µm pore size). We did not choose ultrasonic treatment because we previously demonstrated that this treatment can change the fiber size distribution (*12*). The retained particles were covered with a second layer of carbon. Under this prepared filter, five electron microscopy grids were deposited onto the filtering apparatus. Ten milliliters of chloroform was filtered through the grids to dissolve the Nucleopore filters and retain the fibers, if any, on the grids. We observed the fibers with the transmission electron microscope (Jeol 100CX) at 33,000× magnification. This technique allowed us to determine the quantity of fibers and the volume and the mass that could be calculated with the knowledge of the density (d = 3.35 g/cm^3). Finally, we determined the ratio of the fiber mass to the lung weight (expressed in nanograms per milligram lung).

Lung DNA extraction,* in vitro *packaging, and mutation analysis. We prepared high-molecular-weight lung DNA from a small piece of lung (100 mg) according to the protocol developed by Stratagene (*14*). After homogenization (six strokes in a dounce) using Rnace-it buffer (Stratagene), the DNA samples were phenol/chloroform extracted, then we carefully ethanol precipitated the samples and resuspended them in 500 µL TE (Tris-HCl, 10 mmol, EDTA 1 mmol, pH = 8.0). Before packaging, the DNA was electrophoresed in 1.5% agarose gel to check the size and control the absence of a smear below 50 kB. We recovered the lambda-shuttle vector in viable phage by incubating the extracted DNA (approximately 50 µg) with the terminase and the phage proteins contained in the Transpack (Stratagene) as described by the manufacturer. We matched control and exposed animals for each packaging reaction. The average of plaques per packaging reaction was 38,000, and varied from 19,000 to 69,000. There was no statistical difference for transformation efficiency between control and exposed animals. The *in vitro* packaged phages were adsorbed on *E. coli* SCS-8 cells and screened for blue mutant plaques on 625 cm^2 NYZ agar plates containing 1.5 mg X-gal/ml top agar. The plaque density varied from 8,000 to 10,000 per assay tray. We applied internal color sensitivity control (CM0, CM1, CM2, and CM3; Stratagene) for each plating. Incubation lasted between 16 and 20 hr and the blue mutants were screened using a red filter.

We confirmed the phenotype of each mutant plaque by phage replating at low density in the presence of X-gal. The phage was further isolated by coring the plaque and resuspending the phage in the buffer described in Stratagene's protocol (*14*). We extracted DNA and amplified it with the appropriate primers of the *lacI* gene for further sequencing (forward direction 1781: GACACCATCGAATGGTGAAAAC; reverse direction 1780: CCGCTCACAATTCCACACAACAT). The *lacI* gene of 60 phages from both control and exposed mice was entirely sequenced using the six primer sets recommended in the BigBlue protocol (*14*) to determine the distribution of the mutations. We determined the sequences using the Abi prism dye terminator cycle sequencing ready reaction kit (Perkin Elmer Biosystems, Foster City, CA) on a 373A sequencer (Perkin Elmer Biosystems).

Screening for bulky adducts and determination of m5dC level in DNA. We detected hydrophobic DNA adducts using the [^{32}P]-postlabeling method, which had not previously been used, to check the presence of DNA adducts in asbestos studies. Briefly, the DNA was digested into 3′-phosphonucleosides by micrococcal nuclease and spleen phosphodiesterase. Adducts were privileged versus normal nucleotides by nuclease P_1 enrichment. We postlabeled the adducts using [γ ^{32}P]-adenosine triphosphate (ATP)

and T_4 polynucleotide kinase, as described previously (*15*). The adducts were chromatographed on PEI-cellulose thin-layer plates using four solvents: NaH_2PO_4 2.3 M, pH = 5.7; urea 6.25 M, lithium formate 3.25 M, pH = 3.5; urea 7.5 M, lithium formate 4.25 M, pH= 3.5; and NaH_2PO_4 1.7 M.

For the m5dC determination, we hydrolyzed the DNA into 3′-phosphonucleosides that were labeled directly with γ[^{32}P]-ATP. The resulting [^{32}P]-5′,3′-diphosphonucleosides were further hydrolyzed into [^{32}P]-5′-monophosphate nucleosides by nuclease P_1. The labeled mononucleotides were separated on cellulose plates (F1440; Schleicher and Schüll, Dassel, Germany) and revealed using the solvents as previously mentioned (*15*). We used radioautography to detect the labeled nucleotides and we evaluated the radioactivity using a Bio-Imager Bas2000 analyzer (Fuji, Tokyo, Japan).

Results

Measurement of the fiber concentration in the chamber and in the lung of the mice. We measured the dust concentrations in the chamber by sampling onto glass filters 6 hr/day, as described in "Materials and Methods." The dust concentration mean was 5.75 ± 0.87 mg/m^3. The average fiber density was 1,875 ± 1,216 fibers/cm^3 (n = 24) when we considered only the fibers > 5 µm in length and < 3 µm in diameter. The fiber size distribution was similar to that of a previous study (*12*). The proportion of fiber that met Stanton's criteria (*16*) did not vary over the experiment time and remained < 3% of the overall fibers; thus the crocidolite aerosol used in our study was mainly composed of short fibers (Table 1). The elementary fiber analysis either in the inhalation chamber or in the mice lungs did not show any difference as compared to the initial crocidolite sample (data not shown).

We checked the lung fiber content in four control and four exposed mice 1 week and 12 weeks after the intoxication. No fibers were detected in control mice after either 1 or 12 weeks. Indeed, the measured mass of fiber was < 1 ng/mg lung (Table 2). In contrast, exposed animals had an average of 693 ± 496 ng fibers/mg lung corresponding to 1.63 × 10^6 (± 1.19 × 10^6) fibers/mg lung 1 week after the intoxication. Twelve weeks later, the lung content was still 227 ± 103 ng/mg corresponding to 0.62 × 10^6 (± 0.21 × 10^6) fibers/mg lung. When considering normal breathing of 25 mL/min air, on average, 17.1 and 6.6% of the total inhaled fibers (estimated approximately to 84.4 × 10^6) lasted 1 and 12 weeks, respectively, in the mice lung after the intoxication. The average of the length-on-diameter ratio was 19.15 and 19.88 at 1 and 12 weeks after the exposure, respectively (p > 0.05). Moreover, the fiber size distribution remained unchanged in the lung after 12 weeks and was similar to the fiber size distribution of the aerosol sample (Table 1).

Cellular responses of the bronchoalveolar liquids. Table 3 shows the cellular response of the 1-, 4-, and 12-week series. One week after the intoxication, the number of viable cells elevated dramatically because of a huge increase of PMCs and lymphocytes. However, the number of AMs with two nuclei was approximately 13 times higher in the treated group as compared to the control group. In addition, syncitia composed of three or more macrophages appeared in the exposed group.

Four weeks after the intoxication, only AMs with two or more nuclei were increased. Twelve weeks after the intoxication, the number of AMs was still increased and the AM population was responsible for the increase in total viable cells. The averages of Wagner scores were 1.0 and 1.7 for control and exposed mice, respectively, indicating an alveolar inflammatory response but no fibrosis in the lung (Table 2).

Mutant frequency and mutation spectrum determinations. More than one million genetically independent events were analyzed for each mouse set. We used approximately 55–60 transpack reactions for each time point. The mutant frequency significantly increased 4 weeks after the intoxication: 13.5 × 10^{-5} ± 1.7 × 10^{-5} in the exposed group versus 6.9 × 10^{-5} ± 1.1 × 10^{-5} in the control group (Table 4). The induction factor, defined by the ratio of checked mutants to exposed mice versus checked mutants of control mice, was 1.96 (p < 0.05). In contrast, 1 and 12 weeks after the intoxication, the mutant frequencies of both mice groups were not significantly different.

We determined the mutation spectrum 4 weeks after the exposure for 60 mutant plaques that were sequenced in both groups. Considering the 60 *lacI* genes from mutant plaques sequenced for each group, there were no significant differences between control and exposed mice, as mentioned in Table 5.

We located the mutation positions for both groups (Figure 1). No difference appeared in the location between exposed and control mice (65 and 62 mutations determined, respectively). Similarly, there were no differences in either the 1-week or the 12-week groups (data not shown).

Bulky adducts and methylation status. The formation of bulky DNA adducts was ruled out by the [^{32}P] postlabeling method (*15*). As shown in Figure 2A and B, there

Table 1. Size distribution of the fibers in the exposed animals and of the crocidolite aerosol.

Sample	L < 5 µm	5 µm < L < 20 µm	L > 20 µm	Stanton's fiber[a]	L/D ratio
Treated, 1 week[b]	86.3 ± 5.0	13.6 ± 4.9	0.2 ± 0.3	2.9 ± 1.7	19.15 ± 2.39
Treated, 12 weeks[b]	86.6 ± 2.0	13.1 ± 2.1	0.3 ± 0.2	2.1 ± 0.6	19.88 ± 1.44
Aerosol[c]	91.1	8.4	0.4	2.3	–

Abbreviations: D, diameter; L, length.
[a]L > 8 µm, D < 0.25 µm. [b]n = 4; Rihn et al. (*12*) shows the precise aerosol description. [c]Typical fiber size distribution of an aerosol sample.

Table 2. Fiber load in lung.

Mice group[a]	Lung weight (mg)	Fiber number	Fiber mass (ng/mg)	Wagner scale
Control, 1 week	8.28 ± 0.55	Not detectable	< 1	–
Treated, 1 week	8.86 ± 1.16	1.63 × 10^6 (± 1.19 × 10^6)	693 ± 496	–
Control, 12 weeks	9.38 ± 0.86	Not detectable	< 1	1.0 ± 0.0
Treated, 12 weeks	8.95 ± 0.09	0.62 × 10^6 (± 0.21 × 10^6)	227 ± 103	1.7 ± 0.5

[a]n = 4 for each group.

Table 3. Cellular response of the bronchoalveolar liquid after 1, 4, and 12 weeks after exposure.

Week	Group	AM1	AM2	AM3	PMC	Lymphocytes	Viable cells
1	Control	49,000 ± 19,800	230 ± 190	0 ± 0	490 ± 550	230 ± 270	50,000 ± 20,400
1	Treated	41,100 ± 20,000	3,100 ± 2,100*	800 ± 700*	380,000 ± 390,000*	4,400 ± 3,000*	437,000 ± 390,000*
4	Control	43,700 ± 24,100	320 ± 190	0 ± 0	690 ± 1,000	270 ± 530	45,000 ± 24,300
4	Treated	32,800 ± 10,900	1,900 ± 600*	340 ± 160*	260 ± 320	220 ± 240	34,400 ± 11,900
12	Control	20,900 ± 11,900	120 ± 100	0 ± 0	50 ± 40	0 ± 0	21,500 ± 11,400
12	Treated	44,900 ± 13,400	900 ± 280*	130 ± 100*	120 ± 70	50 ± 60	46,100 ± 13,700*

AM1, AM2, and AM3 are alveolar macrophage with one, two, and three or more nuclei, respectively.
*Significant at p < 0.05 calculated using the Student's t-test (n = 9; three independent measures per animal).

was no difference in the DNA adduct profiles: both exhibited the same adducts, i.e., I-compounds generated by the endogenous metabolism. A slight decrease in the total amount of these I-compounds was detected: 160 versus 60 per 10^9 nucleotides for control and treated mice, respectively. In addition, the m^5dC/dC ratios measured in lung DNA were 3.0 ± 0.7 (n = 16) in control mice versus 3.5 ± 0.4 (n = 16) for the exposed mice. There was no statistical difference in the m^5dC/dC ratio ($p > 0.01$) because it was assessed by radioactivity counting of m^5dC and dC spots on thin-layer chromatography by phosphorimaging.

Discussion

The cumulated dose of asbestos administrated in our study by inhalation was low (5.75 mg/m^3 for 5 days) as compared to previous long-term assays on rodents (10–50 mg/m^3 for 200–500 days) (*17*). Taking into account the average ventilation volume of a mouse, the total inhaled dose of inhaled dust was 0.26 mg/mouse, approximately corresponding to < 0.5% of the average inhaled dose in classical long-term assays. However, it is remarkable that 6.6% of the inhaled dose was still in the lung 12 weeks after the end of the intoxication. Contrary to other studies, there was no overload effect in our study because < 10% (~ 9×10^6) of the total inhaled fibers was present in the lung 4 weeks after the inhalation when the mutagenic effect was significant. The Wagner scores of both groups were similar, indicating that the crocidolite dose was far below the maximum tolerated dose and thus avoiding overload effects (*18*). Moreover, the length/diameter ratio and the size distribution of the fibers deposited in the lung were similar 1 and 12 weeks after a 5-day exposure (Table 1). This similarity shows that in this period of time all fibers, whatever the size, had the same probability to be cleared, which contrasts with long-term assays in which short fibers are removed from the lung more rapidly than long fibers (*19*). It would be interesting to study the mutagenic effect of an asbestos batch composed mainly of long fibers (> 20 µm). Coin et al. (*19*) showed that chrysotile long fibers, which are more carcinogenic (*16*), remained for at least 6 months in the lung after a short treatment comparable to the present study.

Asbestos fibers induce chromosomal changes in human cultured cell lines. Crocidolite and chrysotile (2 mg/cm^2) induced anaphase aberrations and abnormal mitoses in human immortalized mesothelial cell lines (*20*). In human lymphocytes, chromosome and chromatid breaks have also been reported, as well as polyploidy, provided that the dose was higher than 2×10^5 fibers/cm^2 (approximately 5 fibers/cell) (*5*). This dose is higher as compared to the dose used *in vivo* in the present study. Considering a total lung area of 700 cm^2 for a 3-month-old mouse (*13*) and a total number of alveolar type I and II cells of 26×10^6, the number of fibers per cell can be estimated 4 weeks after the intoxication as 0.35 fibers/cell. This value is not surprising because generally the doses needed to show *in vitro* effects are higher than those needed to show *in vivo* effects. After our study, we can conclude that mutations occur using a dose below the dose necessary for chromosome abnormalities. Asbestos fibers also induce binucleation, which is a consequence of mitotic abnormalities in pleural mesothelial cells and macrophages. In the current study, binucleated and multinucleated AMs, known as biomarkers of fiber burden, increase significantly after 4 and 12 weeks: these results were similar to those published previously (*12*).

The first *in vitro* gene mutation assay (i.e., the *Salmonella typhimurium* assay) was not relevant for testing the mutagenicity of crocidolite. An improvement of the Ames test using the TA102 strain showed a mutagenic potential of 50 µg/cm^2 crocidolite because of its sensitivity to oxidative damage (*6*). The hypoxanthine guanine phosphoribosyl transferase locus (*HPRT*) has been investigated in rat liver, Chinese ovary, or human–hamster fibroblasts, but a mutagenic effect of crocidolite could not be demonstrated for any of the the cell systems used [reviewed by Jaurand (*4*)]. Therefore, it appears that the BigBlue transgenic system allows a more realistic picture of the genotoxic effects of an asbestos exposure *in vivo*. In such studies, a nonessential and silent gene, the so-called reporter gene, was used for mutation studies. With this latter system, each point mutation is detected in contrast to assays based on the *HPRT* locus, which are generally phenotypic end points. Recently, however, Park and Aust (*21*) improved the *HPRT* locus assay by using *hprt*$^-$ and *gpt*$^+$ G12 cells where the transgenic *gpt* gene is located on an autosomal chromosome, making this assay useful for asbestos mutagenicity testing. The improved assay showed a 2-fold increase of the mutant frequency with a 6-µg/mL dose of crocidolite.

Recent studies using transgenic rodents exposed to benzo[*a*]pyrene compared the mutant frequencies in both *hprt* and *lacI* genes. The *lacI* genes were 40 times more sensitive to a 150-mg/kg benzo[*a*]pyrene treatment in splenic T cells (*22*). Such disparity could be due to the phenotypic expression of the concerned gene. In fact, *lacI* does not require *in vivo* expression, whereas the resistant 6-thioguanine phenotype (*hprt*$^-$) is required in T cells. Other factors could be the different rate of benzo[*a*]pyrene adduct formation and repair processes in both genes. The *lacI* is a silent gene in the mouse; it is possible that the repair, before translation, is involved in a more efficient manner in the *hprt* gene. Therefore, it appears that a nonexpressed *lacI* transgene is more appropriate to study the genotoxicity of compounds or particles such as asbestos than other end points based on the loss of heterozygosity of the HLA locus or *hprt* phenotyping.

In our study, we sequenced the *lacI* gene using the six primer sets in > 60 mutant colonies isolated from exposed and control mice that represented > 576,000 sequenced bases. We assessed the nature and the position of each mutation. The mutation frequency of control mice in our study varied from 6.9×10^{-5} to 8.7×10^{-5}. These values are slightly higher than the spontaneous mutant frequency determined in lung by de Boer et al. (*23*). This variation could be due to differences in the experimental conditions (e.g., the age of

Table 4. Results of the *in vivo* mutagenesis assay using lung DNA.

Week, group, mouse ID	Plaques (n)	Mutant frequency
One week		
Control		
1	413,130	0.000073
2	367,230	0.000114
3	575,510	0.000075
Mean ± SD		0.000087 ± 0.000023
Total plaques	1,355,870	
Exposed		
4	333,700	0.000093
5	366,620	0.000074
6	423,310	0.000076
Mean ± SD		0.000081 ± 0.000010
Total plaques	1,123,630	
Four weeks		
Control		
7	350,130	0.000080
8	359,040	0.000058
9	350,410	0.000068
Mean ± SD		0.000069* ± 0.000011
Total plaques	1,059,580	
Exposed		
10	409,920	0.000154
11	370,850	0.000124
12	221,880	0.000126
Mean ± SD		0.000135* ± 0.000017
Total plaques	1,002,650	
Twelve weeks		
Control		
13	336,380	0.000134
14	353,870	0.000065
15	364,650	0.000058
Mean ± SD		0.000086 ± 0.000042
Total plaques	1,054,900	
Exposed		
16	351,230	0.000068
17	337,200	0.000184
18	343,500	0.000079
Mean ± SD		0.000110 ± 0.000064
Total plaques	1,031,910	

*Significant ($p < 0.01$, t-test).

the mouse, the plating density, or DNA extraction). Table 5 and Figure 1 show that the mutation spectrum is similar in both groups, suggesting that the increased number of mutations could be due to an oxidative stress directed randomly against all nucleotides rather than to a direct and specific mutagenic effect of fibers, as is seen for initiating compounds such as *o*-anisidine and benzo[*a*]pyrene. The reactive oxygen species (ROS) could be produced by the macrophages and neutrophils burst, as assumed by Hei et al. (*24*), or by extracellular compounds due to fiber surface reactivity (*25–27*). ROS induce mostly deletions and insertions (*28*); Lezon-Geyda et al. (*11*) used an *in vitro* assay based on the same principle (*10*). Moreover, the BigBlue test is unable to detect large insertions and deletions of DNA because these phenomena change the size of the λ phage genome, which cannot be packaged. However an *in vitro* adaptation of the BigBlue system, using cultured Rat 2 λ fibroblasts, allowed Lezon-Geyda et al. (*11*) to demonstrate a 2.5-fold increase of the mitotic recombination after a 6-µg/mL treatment of crocidolite, thus making this test useful for insertion/deletion studies. Although the possibility of mutations through large insertions and deletions cannot be excluded in our test conditions, and because we found a clear increase of the mutant frequency, the exact mutation frequency due to asbestos is probably underestimated.

Table 5. Mutation spectrum.

Mutation type	Control	Treated
Transition		
G:C ⇒ A:T	11 (18.3)	15 (25.4)
A:T ⇒ G:C	4 (6.6)	2 (3.4)
Transversion		
A:T ⇒ T:A	0 (0)	1 (1.7)
A:T ⇒ C:G	2 (3.3)	1 (1.7)
G:C ⇒ T:A	8 (13.3)	7 (11.9)
G:C ⇒ C:G	1 (1.7)	2 (3.4)
Insertion/deletion	30 (50.0)	31 (52.5)
Complex	4 (6.7)	1 (1.7)
Total	60	60
Mutations on CpG sites	10 (16.7)	17 (28.3)

The percentage is indicated in parentheses.

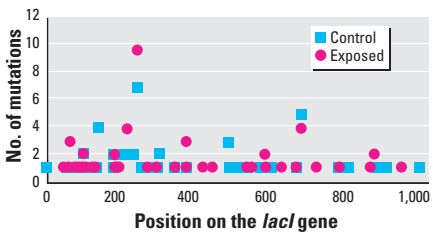

Figure 1. Mutation position on the *lacI* gene. Sixty-five control and 62 treated mutant plaques were sequenced for both mice groups 4 weeks after exposure. For insertion and deletion, only the first modified base was marked.

It is also possible that asbestos impaired the repair potential of the cells, as shown by Okayasu et al. (*29*). An 8-µg/mL dose of chrysotile decreased the cell survival and the double strand repair efficiency of double strand repair deficiency cells (*xrs-5*) as compared to wild-type cells (Chinese hamster ovary cell). The repair potential of DNA was not verified in the present study. Regardless of the mechanism involved, one can hypothesize that the mutant frequency must have increased because of oxidative stress above the repair ability of lung DNA.

McGavran et al. (*30*) showed that a short-term chrysotile exposure (4 mg/m^3) induced cellular proliferation, as assessed by *in vivo* [^{3}H]-thymidine incorporation, in epithelial as well as interstitial lung cells. Adamson (*31*) reported similar findings in lung cells after a single intratracheal administration of 0.1 mg crocidolite. Adamson (*31*) showed a proliferation of mesothelial and fibroblast cells that peaked at 2% labeled nuclei and lasted for 3 weeks. Such an effect was also reported on mesothelial cells in Fischer 344 rats exposed to 8 mg/m^3 crocidolite for 20 days (*32*). Using our experimental design (a moderate dose of 0.26 mg crocidolite for 5 days and a physiologic route for the toxicant), one can hypothesize that a proliferation occurred in lung. Mitogenic factors released in the milieu (*33,34*) by the oxidative stress may fix the mutations shown 4 weeks after the crocidolite exposure. The decrease of the mutant frequency in the exposed mice of the 12-week series could be explained by epithelial regeneration and restored DNA repair after the acute exposure period. The induced cell death could also explain the normalization of the mutant frequency seen after 12 weeks. Indeed, as demonstrated by Broaddus et al. (*25*), a fiber dose of 5 µg/mL induced apoptosis on mesothelial cells in a ROS-induction manner because the apoptosis process was inhibited by extracellular catalase and superoxide dismutase enzymes.

Adachi et al. (*35*) reported an increase of dOH_8dG after an *in vitro* coincubation of deionized crocidolite and DNA. Furthermore, Takeuchi and Morimoto (*36*) showed an increase of this modified nucleotide in HL60 human cells treated with crocidolite and phorbol myristate acetate, a strong mitogenic factor as well as an inducer of ROS. However, they measured the total cell DNA, which could have been contaminated by mitochondrial DNA. dOH_8dG is an early indicator of mitochondrial DNA injury (*37*). Future studies should determine the dOH_8dG level in both nuclear and mitochondrial DNA. In our study, the mutation spectra of both groups of animals showed no statistical difference in the involvement of CpG sites (Table 5). Because mitochondrial DNA represents < 1% of total DNA, our results were not able to reveal a specific increase of this kind of mutation on dG nucleosides therein.

We did not find an excess of adducts in the present study in exposed mice. This is not surprising because the [^{32}P]-postlabeling method detects only the bulky adducts. Inversely, the number of bulky adducts per genome seems more important in the control mice as compared to exposed animals: a similar finding was already noted by Randerath et al. (*38*), who found a gradual depletion of I-compounds during carcinogenesis in rodents. Howden and Faux (*39*) reported the presence of DNA adducts by using a fluorescence technique and demonstrated the role of lipid peroxidation products as malondialdehyde. This *in vitro* paradigm, however, was far from the physiological conditions. Moreover,

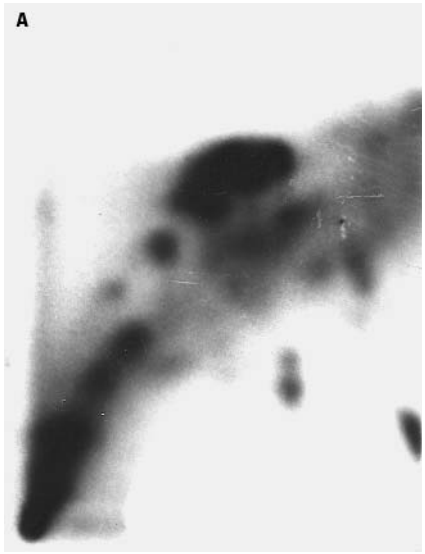

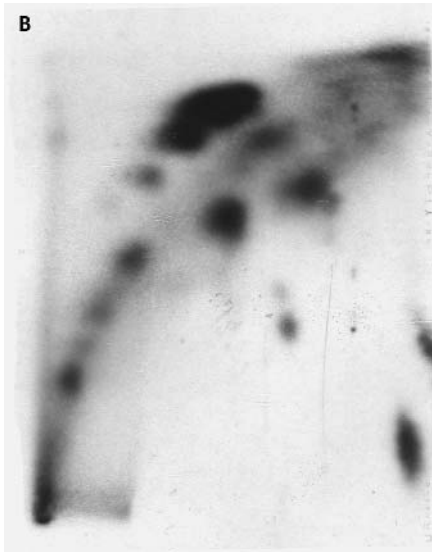

Figure 2. Thin-layer chromatographies of lung DNA adducts of a (*A*) control and (*B*) exposed mouse.

the [^{32}P]-postlabeling method is more sensitive and detected only I-compounds using an *in vivo* paradigm in both exposed and control animals.

Conclusions

We demonstrated a significant increase of the mutant frequency (approximately twice that of the control) of lung DNA for the first time in crocidolite-exposed mice as compared to nonexposed mice. Our study is the first attempt to quantify and qualify the mutagenic potential *in vivo* with respect to a physiologically based and controlled mode of exposure (nose-only inhalation) without overload and with the respect to AM clearance of fibers.

Our study shows that mutagenesis is an early event in fiber intoxication, which could be evoked in cell transformation due to asbestos fibers. In addition, a low dose of fibers, as compared to previous studies, is sufficient to observe mutagenesis *in situ* in lung DNA. The mice paradigm developed in this study should now be experienced with man-made mineral fiber with (e.g., ceramic fibers) and without (e.g., glass fiber) known carcinogenic potential in rodents. It would also be useful to measure the mutant frequency *in vivo* using asbestos of various sizes to correlate, if possible, the mutagenic and the carcinogenic potential of fibers *in vivo*.

References and Notes

1. National Institute for Occupational Safety and Health. Asbestos, Crocidolite. Accession No. CI 6479000. Registry of Toxic Effects of Chemical Substances [CD-ROM]. Hamilton, Ontario, Canada:Canadian Centre for Occupational Health and Safety, December 1999.
2. Kane AB. Mechanism of fiber carcinogenesis. IARC Sci Publ 140:11–34 (1996).
3. Barrett JC, Lamb PW, Wiseman RW. Multiple mechanisms for the carcinogenic effects of asbestos and other mineral fibers. Environ Health Perspect 81:81 (1989).
4. Jaurand MC. Mechanisms of fiber-induced genotoxicity. Environ Health Perspect 105(suppl 5):1073–1084 (1997).
5. Jaurand MC. Mechanisms of fibre carcinogenesis. IARC Sci Publ 140:55–71 (1996).
6. Faux SP, Howden PJ, Levy LS. Iron-dependent formation of 8-hydroxydeoxyguanosine in isolated DNA and mutagenicity in *Salmonella typhimurium* TA102 induced by crocidolite. Carcinogenesis 15:1749–1751 (1994).
7. Hei TK, Piao CQ, He ZY, Vannais D, Waldren CA. Chrysotile fiber is a strong mutagen in mammalian cells. Cancer Res 52:6305–6309 (1992).
8. Kenne K, Ljungquist S, Ringertz NR. Effects of asbestos fibers on cell division, cell survival, and formation of thioguanine-resistant mutants in Chinese hamster ovary cell. Environ Res 39:448–464 (1986).
9. Reiss B, Solomon S, Tong C, Levenstein M, Rosenberg SH, Williams GM. Absence of mutagenic activity of three forms of asbestos in liver epithelial cells. Environ Res 27:389–397 (1982).
10. Both K, Turner DR, Henderson DW. Loss of heterozygosity in asbestos-induced mutations in a human mesothelioma cell line. Environ Mol Mutagen 26:67–71 (1995).
11. Lezon-Geyda K, Jaime CM, Godbold JH, Savransky EF, Hope A, Kheiri SA, Dzmura ZM, Uehara H, Johnson EM, Fasy TM. Chrysotile asbestos fibers mediate homologous recombination in Rat2 lambda fibroblasts: implications for carcinogenesis. Mutat Res 361:113–120 (1996).
12. Rihn B, Kauffer E, Martin P, Coulais C, Villa M, Bottin MC, Vigneron JC, Edorh A, Martinet N. Short-term crocidolite inhalation studies in mice: validation of an inhalation chamber. Toxicology 109:147–156 (1996).
13. Brewer NR. Respiratory physiology. In: The Mouse in Biomedical Research, Vol 3: Normative Biology, Immunology, and Husbandry (Foster HL, Small JD, Fox JG, eds). New York:Academic Press, 1983;252–256.
14. Stratagene. Big Blue® Transgenic Mouse Mutagenesis Assay System, Instruction Manual. La Jolla, CA: Strategene, August 1992.
15. Rihn B, Edorh A, Coulais C, Bottin MC, Keith G. Ethylene glycol monobutyl ether has neither epigenetic nor genotoxic effects in acute treated rats, in subchronic treated v-Ha-*ras* transgenic mice. Occup Hyg 2:237–249 (1996).
16. Stanton MF, Layard M, Tegeris A, Miller E, May M, Morgan E, Smith A. Relation of particle dimension to carcinogenicity in amphibole asbestoses and other fibrous minerals. J Natl Cancer Inst 67(5):965–975 (1981).
17. WHO. Asbestos and Other Natural Mineral Fibers. Environmental Health Criteria 53. Geneva:World Health Organization, 1986;69–107.
18. Oberdörster G. Pulmonary carcinogenicity of inhaled particles and the maximum tolerated dose. Environ Health Perspect 105(suppl 5):1347–1355 (1997).
19. Coin PG, Osornio-Vargas AR, Roggli VL, Brody AR Pulmonary fibrogenesis after three consecutive inhalation exposures to chrysotile asbestos. Am J Respir Crit Care Med 154:1511–1519 (1996).
20. Pelin K, Husgafvel-Pursiainen K, Vallas M, Vanhala E, Linnainmaa K. Cytotoxicity and anaphase aberrations induced by mineral fibers in cultured human mesothelial cells. Toxicol In Vitro 6:445–450 (1992).
21. Park S-H, Aust AE. Participation of iron and nitric oxide in the mutagenicity of asbestos in *hgprt$^-$, gpt$^+$* Chinese hamster V79 cells. Cancer Res 58:1144–1148 (1998).
22. Skopek TR, Kort KL, Marino DR, Mittal LV, Umbenhauer DR, Laws GM, Adams SP. Mutagenic response of the endogenous *hprt* gene and *lacI* transgene in benzo[*a*]pyrene treated Big Blue B6C3F$_1$ mice. Environ Mol Mutagen 28:376–384 (1996).
23. de Boer JG, Provost S, Gorelick N, Tindall K, Glickman BW. Spontaneous mutation in *lacI* transgenic mice: a comparison of tissues. Mutagenesis 13:109–114 (1998).
24. Hei TK, Wu LJ, Piao CQ. Malignant transformation of immortalized human bronchial epithelial cells by asbestos fibers. Environ Health Perspect 105(suppl) 5:1085–1088 (1997).
25. Broaddus VC, Yang L, Scavo LM, Ernst JD, Boylan AM. Crocidolite asbestos induces apoptosis of pleural mesothelial cells: role of reactive oxygen species and poly(ADP-ribosyl) polymerase. Environ Health Perspect 105(suppl 5):1147–1152 (1997).
26. Simeonova PP, Toriumi W, Kommineni C, Erkan M, Munson AE, Rom WN, Luster MI. Molecular regulation of IL-6 activation by asbestos in lung epithelial cells: role of reactive oxygen species. J Immunol 159:3921–3928 (1997).
27. Schapira RM, Ghio AJ, Effros RM, Morrisey J, Dawson CA, Hacker AD. Hydroxyl radicals are formed in the rat lung after asbestos instillation in vivo. Am J Respir Cell Mol Biol 10:573–579 (1994).
28. Hsie AW, Xu Z, Yu Y, Sonier MA, Hrelia P. Molecular analysis of reactive oxygen-species-induced mammalian gene mutation. Teratogen Carcinog Mutagen 10:115–124 (1990).
29. Okayasu R, Takahashi S, Yamada S, Hei TK, Ulrich RL. Asbestos and double strand breaks. Cancer Res 59:298–300 (1999).
30. McGavran PD, Moore LB, Brody AR. Inhalation of chrysotile asbestos induces rapid cellular proliferation in small pulmonary vessels of mice and rats. Am J Pathol 136:695–705 (1990).
31. Adamson IY. Early mesothelial cell proliferation after asbestos exposure: *in vivo* and *in vitro* studies. Environ Health Perspect 105(suppl 5):1205–1208 (1997).
32. BéruBé KA, Quinlan TR, Moulton G, Hemenway D, O'Shaughnessy P, Vacek P, Mossman BT. Comparative proliferative and histopathologic changes in rat lungs after inhalation of chrysotile or crocidolite asbestos. Toxicol Appl Pharmacol 137:67–74 (1996).
33. Osier M, Baggs RB, Oberdörster G. Intratracheal instillation versus intratracheal inhalation: influence of cytokines on inflammatory response. Environ Health Perspect 105(suppl 5):1265–1271 (1997).
34. Finkelstein JN, Johnston C, Barrett T, Oberdörster G. Particulate-cell interactions and pulmonary cytokine expression. Environ Health Perspect 105(suppl 5):1179–1182 (1997).
35. Adachi S, Yoshida S, Kawamura K, Takahashi M, Uchida H, Odagiri Y, Takemoto K. DNA damage and mesothelioma by crocidolite, with special reference to the presence of iron inside and outside of asbestos fiber. Carcinogenesis 15:753–758 (1994).
36. Takeuchi T, Morimoto K. Crocidolite asbestos increased 8-hydroxydeoxyguanosine levels in cellular DNA of a human promyelocytic leukemia cell line, HL60. Carcinogenesis 15:635–639 (1994).
37. Salazar JJ, Van Houten B. Preferential mitochondrial DNA injury caused by glucose oxidase as a steady generator of hydrogen peroxide in human fibroblasts. Mutat Res 385:139–149 (1997).
38. Randerath K, Chang J, Randerath E. Age dependent DNA modifications (I-compounds): effects of carcinogenesis and oxidative stress. In: Oxidative Stress and Aging (Cutler RG, Packer L , Bertram J, Mori A, eds). Basel:Birkhäuser Verlag, 1995;77–87.
39. Howden PJ, Faux SP. Fibre-induced lipid peroxidation leads to DNA adduct formation in *Salmonella typhimurium* TA104 and rat lung fibroblasts. Carcinogenesis 17:413–419 (1996).